

## Chapter 2

# Flow and Functional Models for Rheological Properties of Fluid Foods

A flow model may be considered to be a mathematical equation that can describe rheological data, such as shear rate versus shear stress, in a basic shear diagram, and that provides a convenient and concise manner of describing the data. Occasionally, such as for the viscosity versus temperature data during starch gelatinization, more than one equation may be necessary to describe the rheological data. In addition to mathematical convenience, it is important to quantify how magnitudes of model parameters are affected by state variables, such as temperature, and the effect of structure/composition (e.g., concentration of solids) of foods and establish widely applicable relationships that may be called functional models.

Rheological models may be grouped under the categories: (1) empirical, (2) theoretical, and (3) structural. Obviously, an empirical model, such as the power law (Eq. 2.3), is deduced from examination of experimental data. A theoretical model is derived from fundamental concepts and it provides valuable guidelines on understanding the role of structure. It indicates the factors that influence a rheological parameter. The Krieger–Dougherty model (Krieger 1985) (Eq. 2.26) for relative viscosity is one such model. Another theoretical model is that of Shih et al. (1990) that relates the modulus to the fractal dimension of a gel.

A structural model is derived from considerations of the structure and often kinetics of changes in it. It may be used, together with experimental data, to estimate values of parameters that help characterize the rheological behavior of a food sample. One such model is that of Casson (Eq. 2.6) that has been used extensively to characterize the characteristics of foods that exhibit yield stress. Another structural model is that of Cross (1965) (Eq. 2.14) that has been used to characterize flow behavior of polymer dispersions and other shear-thinning fluids. While application of structure-based models to rheological data provides useful information, structure-based analysis can provide valuable insight in to the role of the structure of a dispersed system. For example, as discussed in Chap. 5, it allows for estimating the contributions of interparticle bonding and network of particles of dispersed systems.

Flow models have been used also to derive expressions for velocity profiles and volumetric flow rates in tube and channel flows, and in the analysis of heat transfer phenomenon. Numerous flow models can be encountered in the rheology literature

**Table 2.1** Some two- and three-parameter flow models for describing shear rate ( $\dot{\gamma}$ ) versus shear stress ( $\sigma$ ) data

$\sigma = \eta \dot{\gamma}$	Newtonian model*
$\sigma = \frac{\dot{\gamma}}{\left[ \frac{1}{\eta_0} + K_E (\sigma)^{(1/\eta_E)-1} \right]}$	Ellis model for low-shear rate data containing $\eta_0$ (Brodkey 1967)
$\sigma = \left[ \eta_\infty \dot{\gamma} + K_s \dot{\gamma}^{n_s} \right]$	Sisko model for high-shear rate data containing $\eta_\infty$ (Brodkey 1967)
$\eta_a = \eta_\infty + \frac{\eta_0 - \eta_\infty}{1 + (\alpha_c \dot{\gamma})^m}$	Cross model for data over a wide range of shear rates*
$\eta_a = \eta_\infty + \frac{\eta_0 - \eta_\infty}{[1 + (\lambda_c \dot{\gamma})^2]^N}$	Carreau model for data over a wide range of shear rates*
$\sigma = K \dot{\gamma}^n$	Power law model used extensively in handling applications*
$\sigma - \sigma_0 = \eta' \dot{\gamma}$	Bingham model*
$\sigma - \sigma_{0H} = K_K \dot{\gamma}^{n_H}$	Herschel–Bulkley model*
$\sigma^{0.5} = K_{0c} + K_c (\dot{\gamma})^{0.5}$	Casson model used especially in treating data on chocolates*
$\sigma^{0.5} - \sigma_{0M} = K_M \dot{\gamma}^{n_M}$	Mizrahi and Berk (1972) model is a modification of the Casson model
$\sigma^{n_1} = \sigma_0^{n_1} + \eta_\infty (\dot{\gamma})^{n_2}$	Generalized model of Ofoli et al. (1987)*
$\sigma = [(\sigma_{0V})^{1/n_V} + K_V \dot{\gamma}]^{n_V}$	Vocadlo (Vocadlo and Moo Young 1969) model

\*Discussed in text

and some from the food rheology literature are listed in Table 2.1. Also, here those models that have found extensive use in the analysis of the flow behavior of fluid foods are discussed. Models that account for yield stress are known as viscoplastic models (Bird et al. 1982). For convenience, the flow models can be divided in to those for time-independent and for time-dependent flow behavior.

## Time-Independent Flow Behavior

### Newtonian Model

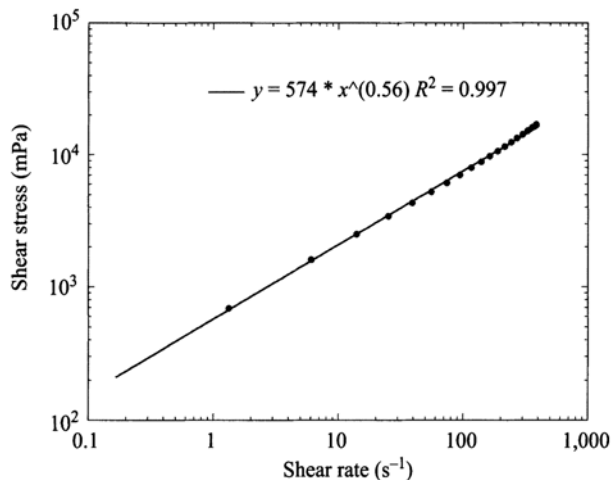
The model for a Newtonian fluid is described by the equation:

$$\sigma = \eta \dot{\gamma} \quad (2.1)$$

As per the definition of a Newtonian fluid, the shear stress,  $\sigma$ , and the shear rate,  $\dot{\gamma}$ , are proportional to each other, and a single parameter,  $\eta$ , the viscosity, characterizes the data. For a Bingham plastic fluid that exhibits a yield stress,  $\sigma_0$ , the model is:

$$\sigma - \sigma_0 = \eta' \dot{\gamma} \quad (2.2)$$

**Fig. 2.1** Plot of log shear rate ( $\dot{\gamma}$ ) versus log shear stress ( $\sigma$ ) for a 2.6% Tapioca starch dispersion heated at 67°C for 5 min (Tattiyakul 1997) to illustrate applicability of the power law model



where,  $\eta'$  is called the Bingham plastic viscosity.

As shown in Fig. 2.1, the Newtonian model and the Bingham plastic model can be described by straight lines in terms of shear rate and shear stress, and the former can be described by one parameter  $\eta$  and the latter by two parameters:  $\eta'$  and  $\sigma_0$ , respectively. However, the shear rate–shear stress data of shear-thinning and shear-thickening fluids are curves that require more than one parameter to describe their data. Given that the equation of a straight line is simple, it is easy to understand attempts to transform shear rate–shear stress data in to such lines. An additional advantage of a straight line is that it can be described by just two parameters: the slope and the intercept.

### Power Law Model

Shear stress–shear rate plots of many fluids become linear when plotted on double logarithmic coordinates and the power law model describes the data of shear-thinning and shear thickening fluids:

$$\sigma = K \dot{\gamma}^n \quad (2.3)$$

where,  $K$  the consistency coefficient with the units: Pa s <sup>$n$</sup>  is the shear stress at a shear rate of 1.0 s<sup>-1</sup> and the exponent  $n$ , the flow behavior index, is dimensionless that reflects the closeness to Newtonian flow. The parameter  $K$  is sometimes referred to as consistency index. For the special case of a Newtonian fluid ( $n=1$ ), the consistency index  $K$  is identically equal to the viscosity of the fluid,  $\eta$ . When the magnitude of  $n < 1$  the fluid is shear-thinning and when  $n > 1$  the fluid is shear-thickening in nature. Taking logarithms of both sides of Eq. 2.3:

$$\log \sigma = \log K + n \log \dot{\gamma} \quad (2.4)$$

The parameters  $K$  and  $n$  are determined from a plot of  $\log \sigma$  versus  $\log \dot{\gamma}$ , and the resulting straight line's intercept is  $\log K$  and the slope is  $n$ . If a large number of  $\sigma$  versus  $\dot{\gamma}$  data points, for example,  $>15$  (it is easy to obtain large number of points with automated viscometers) are available, linear regression of  $\log \dot{\gamma}$  versus  $\log \sigma$  will provide statistically best values of  $K$  and  $n$ . Nevertheless, a plot of experimental and predicted values of  $\log \dot{\gamma}$  and  $\log \sigma$  is useful for observing trends in data and ability of the model to follow the data. Figure 2.1 illustrates applicability of the power law model to a 2.6% tapioca starch dispersion heated at 67°C for 5 min. Linear regression techniques also can be used for determination of the parameters of the Herschel–Bulkley (when the magnitude of the yield stress is known) and the Casson models discussed later in this chapter.

Because it contains only two parameters ( $K$  and  $n$ ) that can describe shear rate–shear stress data, the power law model has been used extensively to characterize fluid foods. It is also the most used model in studies on handling of foods and heating/cooling of foods. Extensive compilations of the magnitudes of power law parameters can be found in Holdsworth (1971, 1993). Because it is convenient to group foods in to commodities, a compilation of magnitudes of power law parameters of several food commodities are given in Chap. 5. In addition, the influence of temperature in quantitative terms of activation energies, and the effect of concentration of soluble and insoluble solids on the consistency index are given.

Although the power law model is popular and useful, its empirical nature should be noted. One reason for its popularity appears to be due to its applicability over the shear rate range:  $10^1 - 10^4 \text{ s}^{-1}$  that can be obtained with many commercial viscometers. Often, the magnitudes of the consistency and the flow behavior indexes of a food sample depend on the specific shear rate range being used so that when comparing the properties of different samples an attempt should be made to determine them over a specific range of shear rates. One drawback of the power law model is that it does not describe the low-shear and high-shear rate constant-viscosity data of shear-thinning foods.

### ***Herschel–Bulkley Model***

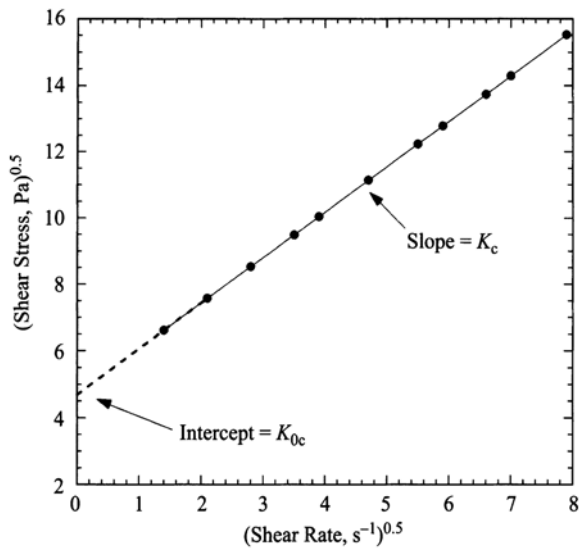
When yield stress of a food is measurable, it can be included in the power law model and the model is known as the Herschel–Bulkley model:

$$\sigma - \sigma_{0H} = K_H \dot{\gamma}^{n_H} \quad (2.5)$$

where,  $\dot{\gamma}$  is shear rate ( $\text{s}^{-1}$ ),  $\sigma$  is shear stress (Pa),  $n_H$  is the flow behavior index,  $K_H$  is the consistency index, and  $\sigma_{0H}$  is yield stress. It is noted here that the concept of yield stress has been challenged (Barnes and Walters 1989) because a fluid may deform minutely at stress values lower than the yield stress. Nevertheless, yield stress may be considered to be an engineering reality and plays an important role in many food products.

If the yield stress of a sample is known from an independent experiment,  $K_H$  and  $n_H$  can be determined from linear regression of  $\log \sigma - \sigma_{0H}$  versus  $\log(\dot{\gamma})$  as

**Fig. 2.2** Plot of  $(\dot{\gamma})^{0.5}$  versus  $(\sigma)^{0.5}$  for a food that follows the Casson model. The square of the intercept is the yield stress and that of slope is the Casson plastic viscosity



the intercept and slope, respectively. Alternatively, nonlinear regression technique was used to estimate  $\sigma_{0H}$ ,  $K_H$ , and  $\eta_H$  (Rao and Cooley 1983). However, estimated values of yield stress and other rheological parameters should be used only when experimentally determined values are not available. In addition, unless values of the parameters are constrained a priori, nonlinear regression provides values that are the best in a least squares sense and may not reflect the true nature of the test sample.

## Casson Model

The Casson model (Eq. 2.6) is a structure-based model (Casson 1959) that, although was developed for characterizing printing inks originally, has been used to characterize a number of food dispersions:

$$\sigma^{0.5} = K_{0c} + K_c(\dot{\gamma})^{0.5} \quad (2.6)$$

For a food whose flow behavior follows the Casson model, a straight line results when the square root of shear rate,  $(\dot{\gamma})^{0.5}$ , is plotted against the square root of shear stress,  $(\sigma)^{0.5}$ , with slope  $K_c$  and intercept  $K_{0c}$  (Fig. 2.2). The Casson yield stress is calculated as the square of the intercept,  $\sigma_{0c} = (K_{0c})^2$  and the Casson plastic viscosity as the square of the slope,  $\eta_{ca} = (K_c)^2$ . The data in Fig. 2.2 are of Steiner (1958) on a chocolate sample. The International Office of Cocoa and Chocolate has adopted the Casson model as the official method for interpretation of flow data on chocolates. However, it was suggested that the vane yield stress would be a more reliable measure of the yield stress of chocolate and cocoa products (Servais et al. 2004).

The Casson plastic viscosity can be used as the infinite shear viscosity,  $\eta_\infty$ , (Metz et al. 1979) of dispersions by considering the limiting viscosity at infinite shear rate:

$$\left( \frac{d\sigma}{d\dot{\gamma}} \right)_{\dot{\gamma} \rightarrow \infty} = \left( \frac{d(\sqrt{\sigma})}{d\dot{\gamma}} \frac{d\sigma}{d(\sqrt{\sigma})} \right)_{\dot{\gamma} \rightarrow \infty} \quad (2.7)$$

Using the Casson equation the two terms in the right-hand side bracket can be written as:

$$\frac{d(\sqrt{\sigma})}{d\dot{\gamma}} = \frac{K_c}{2\sqrt{\dot{\gamma}}} \quad (2.8)$$

and

$$\frac{d\sigma}{d(\sqrt{\sigma})} = 2\sqrt{\sigma} \quad (2.9)$$

Combining the above two equations,

$$\eta_\infty = \eta_{Ca} = (K_c)^2 \quad (2.10)$$

### ***Quemada Model***

Quemada et al. (1985) proposed a viscosity equation for dispersed systems based on zero-shear,  $\eta_0$ , and infinite-shear,  $\eta_\infty$ , viscosities, and a structural parameter,  $\lambda$ , dependent on the shear rate, that may be written as:

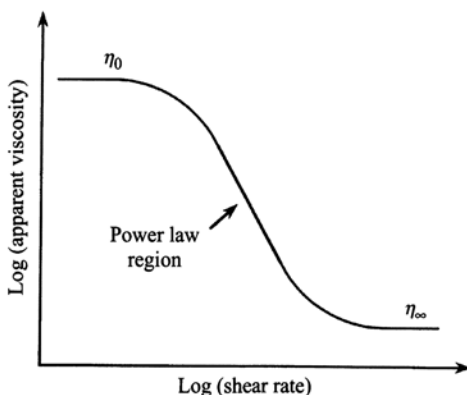
$$\frac{\eta}{\eta_\infty} = \frac{1}{\left\{ 1 - \left[ 1 - \left( \frac{\eta_\infty}{\eta_0} \right)^{0.5} \right] \lambda \right\}^2} \quad (2.11)$$

where,

$$\lambda = \frac{1}{[1 + (t_c \dot{\gamma})^{0.5}]} \quad (2.12)$$

The time constant  $t_c$  is related to the rate of aggregation of particles due to Brownian motion. For highly concentrated dispersed systems,  $\eta_\infty$  will be much lower than  $\eta_0$ , so that  $(\eta_\infty/\eta_0) \ll 1$  and the dispersion may have a yield stress, and Eq. (2.11) reduces to the Casson model (Eq. 2.6) (Tiu et al. 1992) with the Casson yield stress,  $\sigma_{0c} = (\eta_\infty/t_c)$ . Thus the Casson–Quemada models can be used to examine dispersions whose rheological behaviors range from only shear-thinning to shear thinning with yield stress. The Casson–Quemada models were used to study the role of cocoa sol-

**Fig. 2.3** Plot of shear rate versus apparent viscosity for shear thinning foods identifying three separate regions: a zero-shear viscosity at low shear rates, a power law region at intermediate shear rates, and an infinite-shear viscosity at high-shear rates. Often, only data in the power law region are obtained



ids and cocoa butter on cocoa dispersions (Fang et al. 1996, 1997) to be discussed in Chap. 5.

A general model for shear rate–shear stress data that under specific assumptions reduces to the Herschel–Bulkley, the Casson, and other models was presented by Ofoli et al. (1987):

$$\sigma^{n_1} = \sigma_0^{n_1} + \eta_{\infty} (\dot{\gamma})^{n_2} \quad (2.13)$$

where,  $n_1$  and  $n_2$  are constants, and  $\eta_{\infty}$  is the infinite shear viscosity. It is important to note that one model may be applicable at low-shear rates and another at high-shear rates (Dervisoglu and Kokini 1986). While applicability of the flow models themselves may be interesting, it is much more important to study the role of food composition on a model's parameters and apply the model to better understand the nature of foods.

## Apparent Viscosity—Shear Rate Relationships of Shear-Thinning Foods

At sufficiently high polymer concentrations, most shear-thinning biopolymer (also called a gum or a hydrocolloid) dispersions exhibit similar three-stage viscous response when sheared over a wide shear rate range (Fig. 2.3): (1) at low-shear rates, they show Newtonian properties with a constant zero-shear viscosity ( $\eta_0$ ) over a limited shear range that is followed by, (2) a shear-thinning range where solution viscosity decreases in accordance with the power law relationship; the reciprocal of the shear rate at which the transition from Newtonian to pseudoplastic behavior occurs is the characteristic time or the time constant, and (3) attains a limiting and constant infinite-shear-viscosity ( $\eta_{\infty}$ ). The three regions may be thought of being

due rearrangement in the conformation of the biopolymer molecules in the dispersion due to shearing. In stage 1 when the magnitude of  $\dot{\gamma}$  is low, there is little rearrangement of the polymer chains, while in stage 2 the chains undergo gradual rearrangement with  $\dot{\gamma}$  resulting in a power law behavior. In stage 3, the shear rate is sufficiently high that the polymer chains do not undergo much rearrangement.

### ***Cross and Carreau Models***

The apparent viscosity ( $\eta_a$ ) of the solution can be correlated with shear rate ( $\dot{\gamma}$ ) using the Cross (Eq. 2.14) or the Carreau (Eq. 2.15) equations, respectively.

$$\eta_a = \eta_\infty + \frac{\eta_0 - \eta_\infty}{1 + (\alpha_c \dot{\gamma})^m} \quad (2.14)$$

$$\eta_a = \eta_\infty + \frac{\eta_0 - \eta_\infty}{[1 + (\lambda_c \dot{\gamma})^2]^N} \quad (2.15)$$

where,  $\alpha_c$  and  $\lambda_c$  are time constants related to the relaxation times of the polymer in solution and  $m$  and  $N$  are dimensionless exponents. Because magnitudes of  $\eta_\infty$  of food polymer dispersions with concentrations of practical interest are usually very low in magnitude, they are difficult to determine experimentally. Therefore, to avoid consequent errors in estimation of the other rheological parameters in Eqs. 2.14 and 2.15, often  $\eta_\infty$  has been neglected (Abdel-Khalik et al. 1974; Lopes da Silva et al. 1992). The Cross and Carreau models described well the shear dependence of aqueous dispersions of high methoxyl pectins and locust bean gum (Lopes da Silva et al. 1992), konjac flour gum (Jacon et al. 1993), and mesquite gum solution (Yoo et al. 1995), and other gums (Launay et al. 1986). In general, the model of Cross has been used in studies in Europe and that of Carreau in North America. In Chap. 4, the applicability of the Cross and Carreau models to locust bean gum dispersions will be discussed in more detail.

For small values of  $\eta_\infty$ , the Cross exponent  $m$  tends to a value  $(1-n)$ , where  $n$  is the power law flow behavior index (Launay et al. 1986; Giboreau et al. 1994). For the shear rate,  $\dot{\gamma}_c$  where  $\eta_{ap} = (\eta_0 + \eta_\infty)/2$ , the Cross time constant  $\alpha_c = 1/\dot{\gamma}_c$ . Generally,  $\dot{\gamma}_c$  gives an order of magnitude of the critical shear rate marking the end of the zero shear rate Newtonian plateau or the onset of the shear-thinning region. It is therefore important to recognize the shear rate dependence of the rheological behavior of polysaccharide polymers in solution and the difficulty involved in obtaining experimental data over the applicable shear rate range of  $10^{-6} - 10^4 \text{ s}^{-1}$  (Barnes et al. 1989). The low-shear rate region of about  $10^{-3} - 10^0$  is often used for the characterization and differentiation of structures in polysaccharide systems through the use of stress controlled creep and non destructive oscillatory tests. The shear rate range of about  $10^1 - 10^4 \text{ s}^{-1}$  falls within the operational domain of most commercial



rheometers, so that the range of  $10^{-3} - 10^4 \text{ s}^{-1}$  can sometimes be effectively covered by a combination of measuring procedures and instruments.

Both the Carreau and the Cross models can be modified to include a term due to yield stress. For example, the Carreau model with a yield term given in Eq. (2.16) was employed in the study of the rheological behavior of glass-filled polymers (Poslinski et al. 1988):

$$\eta_a = \sigma_0 \dot{\gamma}^{-1} + \eta_p [1 + (\lambda_p \dot{\gamma})^2]^{-N} \quad (2.16)$$

where,  $\sigma_0$  is the yield stress,  $\eta_p$  is the plateau viscosity, and  $\lambda_p$  and  $N$  are constants to be determined from experimental data. Rayment et al. (1998) interpreted the rheological behavior of guar gum dispersions containing raw rice starch in terms of the Cross model with yield stress (Eq. 2.17). We note that, when yield stress is exhibited, the term plateau viscosity is used instead of zero-shear viscosity:

$$\eta_a = \sigma_0 \dot{\gamma}^{-1} + \eta_p [1 + (\alpha_c \dot{\gamma})]^{-m} \quad (2.17)$$

## Models for Time-Dependent Flow Behavior

Considerable care should be exercised in determining reliable time-dependent rheological data because of the often unavoidable modification in structure due to sample handling and during loading the sample in a viscometer or rheometer measuring geometry. Nevertheless, with careful attention to details, such as allowing a sample to relax in the rheometer measuring geometry, rheological data can be obtained to characterize time-dependent rheological behavior.

### *Weltman Model*

The Weltman (1943) model has been used to characterize thixotropic (Paredes et al. 1988) behavior and of antithixotropic behavior (da Silva et al. 1997) of foods:

$$\sigma = A - B \log t \quad (2.18)$$

where,  $\sigma$  is shear stress (Pa),  $t$  is time (s), and  $A$  (value of stress at  $t=1$  s) and  $B$  are constants. A plot of  $\sigma$  versus log time should result in a straight line. In thixotropic behavior  $B$  takes negative values and in antithixotropic behavior it takes positive values. Table 2.2 shows typical magnitudes of the constants  $A$  and  $B$  for cross-linked waxy maize starch dispersions.

**Table 2.2** Weltman Equation parameters for cross-linked waxy maize gelatinized starch dispersions. (Da Silva et al. 1997)

Weltman Parameter	Conc. (%)	Shear rate (s <sup>-1</sup> )			
		50	100	200	300
A	3	$6.97 \times 10^{-2}$	$5.76 \times 10^{-2}$	$4.22 \times 10^{-2}$	
	4	$2.97 \times 10^{-1}$	$2.08 \times 10^{-1}$	$1.72 \times 10^{-1}$	$9.54 \times 10^{-2}$
	5		$5.39 \times 10^{-1}$	$3.88 \times 10^{-1}$	$3.55 \times 10^{-1}$
B	3	$1.58 \times 10^{-3}$	$5.71 \times 10^{-4}$	$1.66 \times 10^{-5}$	
	4	$3.15 \times 10^{-3}$	$2.07 \times 10^{-3}$	$5.29 \times 10^{-3}$	$7.83 \times 10^{-3}$
	5		$8.30 \times 10^{-5}$	$1.06 \times 10^{-2}$	$8.79 \times 10^{-3}$
Correlation coef.	3	1.00	1.00	1.00	
	4	1.00	1.00	1.00	1.00
	5		1.00	1.00	1.00

### *Tiu–Boger Model*

A model to study thixotropic behavior of foods exhibiting yield stress was devised by Tiu and Boger (1974) who studied the time-dependent rheological behavior of mayonnaise by means of a modified Herschel–Bulkley model:

$$\sigma = \lambda \left[ \sigma_{0H} + K_H (\dot{\gamma})^{n_H} \right] \quad (2.19)$$

where,  $\sigma$  is the shear stress (Pa),  $\dot{\gamma}$  is the shear rate (s<sup>-1</sup>),  $\lambda$  is a time-dependent structural parameter that ranges from an initial value of unity to an equilibrium value  $\lambda_e$ ,  $\sigma_{0H}$  is the yield stress (Pa),  $K_H$  is the consistency index (Pa s<sup>n</sup>), and  $n_H$  is the flow behavior index. The decay of the structural parameter with time was assumed to obey a second-order equation:

$$\frac{d\lambda}{dt} = -k_1 (\lambda - \lambda_e)^2 \quad (2.20)$$

where, the constant  $k_1$  is a function of shear rate to be determined experimentally. While the determination of  $\sigma_{0H}$ , and  $n_H$  is straight forward, estimation of  $k_1$  and  $\lambda_e$  requires the use of values of apparent viscosities ( $\eta_a$ ) (Tiu and Boger 1974):

$$\lambda = \frac{\eta_a \dot{\gamma}}{\sigma_{0H} + K_H \dot{\gamma}^{n_H}} \quad (2.21)$$

and

$$\frac{d\eta_a}{dt} = -a_1 (\eta_a - \eta_e)^2 \quad (2.22)$$

Rheology of Fluid, Semisolid, and Solid Foods

Principles and Applications

Rao, M.A.

2014, XIII, 461 p. 202 illus., 1 illus. in color., Hardcover

ISBN: 978-1-4614-9229-0